

This document is downloaded from DR-NTU, Nanyang Technological University Library, Singapore.

Title	Estimation of strength, permeability and hydraulic diffusivity of Pozzolana blended concrete through pore size distribution
Author(s)	Kondraivendhan, B.; Divsholi, Bahador Sabet; Teng, Susanto
Citation	Kondraivendhan, B., Divsholi, B. S., & Teng, S. (2013). Estimation of strength, permeability and hydraulic diffusivity of Pozzolana blended concrete through pore size distribution. <i>Journal of advanced concrete technology</i> , 11(9), 230-237.
Date	2013
URL	<a href="http://hdl.handle.net/10220/23929">http://hdl.handle.net/10220/23929</a>
Rights	© 2013 Japan Concrete Institute. This paper was published in <i>Journal of Advanced Concrete Technology</i> and is made available as an electronic reprint (preprint) with permission of Japan Concrete Institute. The paper can be found at the following official DOI: <a href="http://dx.doi.org/10.3151/jact.11.230">http://dx.doi.org/10.3151/jact.11.230</a> . One print or electronic copy may be made for personal use only. Systematic or multiple reproduction, distribution to multiple locations via electronic or other means, duplication of any material in this paper for a fee or for commercial purposes, or modification of the content of the paper is prohibited and is subject to penalties under law.



## **Estimation of strength, permeability and hydraulic diffusivity of pozzolana blended concrete through pore size distribution**

B. Kondraivendhan , B. Sabet Divsholi, Susanto Teng

*Journal of Advanced Concrete Technology*, volume 11 (2013 ), pp. 230-237

### **Related Papers** [Click to Download full PDF!](#)

#### **Modeling the Influence of Pore Structure on the Acoustic Absorption of Enhanced Porosity Concrete**

Narayanan Neithalath, Adam Marolf, Jason Weiss, Jan Olek

*Journal of Advanced Concrete Technology*, volume 3 (2005), pp. 29-40

#### **Characterizing the 3D Pore Structure of Hardened Cement Paste with Synchrotron Microtomography**

Michael J. P. Promentilla, Takafumi Sugiyama, Takashi Hitomi, Nobufumi Takeda

*Journal of Advanced Concrete Technology*, volume 6 (2008), pp. 273-286

#### **Pore Structure Model of Hydrates Comprising Various Cements and SCMs Based on Changes in Particle Size of Constituent Phases**

Yusuke Fujikura, Hideki Oshita

*Journal of Advanced Concrete Technology*, volume 9 (2011), pp. 133-147

#### **Correlation between Permeability of Concrete and Threshold Pore Size Obtained with Epoxy-coated Sample**

Yuya Sakai, Choji Nakamura, Toshiharu Kishi,

*Journal of Advanced Concrete Technology*, volume 11 (2013), pp. 189-195

[Click to Submit your Papers](#)

Japan Concrete Institute <http://www.j-act.org>



## Scientific paper

# Estimation of Strength, Permeability and Hydraulic Diffusivity of Pozzolana Blended Concrete Through Pore Size Distribution

B. Kondraivendhan<sup>1</sup>, B. Sabet Divsholi<sup>2</sup> and Susanto Teng<sup>3</sup>

Received 2 November 2012, accepted 9 September 2013

doi:10.3151/jact.11.230

## Abstract

The compressive strength, permeability and hydraulic diffusivity of Ordinary Portland Cement (OPC) with or without pozzolana blended concrete have been estimated in this investigation by using Mercury Intrusion Porosimetry (MIP). With this in view, concrete cubical specimens were crushed and the broken chunks with aggregates were collected from different mixes such as OPC mix, OPC with silica fume (5%, 10% and 15% of replacements) mix and OPC with slag (10%, 30% and 50% of replacements) mixes. The MIP experimentation was carried out for wide range of curing ages such as 1, 3, 7, 28, 42 and 90 days. The experimental Pore Size Distribution (PSD) parameters such as mean distribution radius ( $r_{0.5}$ ), dispersion coefficient ( $d$ ) and permeable porosity ( $P$ ) for all mixes were calculated by using the Morgan Mercer Flodin (MMF) model. The application of experimental PSD parameters is demonstrated by estimating the compressive strength, permeability and hydraulic diffusivity through the readily available corresponding relationships in the literature. It is observed that the lowest  $r_{0.5}$  and high  $d$  values are obtained in case of OPC with silica fume mix as compared to other mixes owing to its better pore refinement. It is observed that the estimated permeability increases with an increase in w/c ratio and decreases with an increase in curing ages which resembles the trend of Powers' permeability versus w/c ratio curves.

## 1. Introduction

Concrete is the most widely used construction material around the world. It is a composite material with a complex structure. At the macroscopic level, concrete may be considered to be a two-phase material, consisting of aggregate particles dispersed in a matrix of the cement paste. At the microscopic level apart from aggregate phase and Hydrated Cement Paste (HCP) phase, a third phase known as the interfacial transition zone (ITZ) comes into picture. In the past few decades, concrete research has been focussed at the microscopic level i.e. the internal microstructure of cement based materials. The microstructure generally governs the strength and durability of cement based materials. The microstructure consists of hardened cement based materials with residual pore system (Nagaraj and Zahinda 1996). The pore system consists of porosity and pore sizes. The pore size characteristics of the porous material are generally represented by pore size distribution either in the form of cumulative pore size distribution or differential pore size distribution. A general form PSD curve has been

proposed by Patil and Bhattacharjee (2008) that involves porosity ( $P$ ), mean distribution radius ( $r_{0.5}$ ) corresponding to 50% of cumulative intruded pore volume and dispersion coefficient ( $d$ ).

There are many methods to measure the porosity and pore size distribution such as fluid displacement method, Helium pycnometer, capillary condensation and adsorption desorption isotherm, small angle x-ray scattering (SAXS) method, scanning electron microscope (SEM), nuclear magnetic resonance (NMR), AC impedance spectroscopy, mercury intrusion porosimetry (MIP) and back scattered electron images (BSE) (Patil 2006). Among these methods, MIP is the most popular method (Bhattacharjee and Krishnamoorthy 2004).

Pores of all types and shapes (gel pores, capillary pores, compaction pores and pores in the ITZ) control the strength and mechanical properties of concrete (Kumar and Bhattacharjee 2003), the durability performances are mainly controlled by the interconnected pores. Larger pores are known to have dominant effect on the strength and durability compared to gel pores which are known to affect the shrinkage and creep (Kumar and Bhattacharjee 2004). Thus, knowledge of porosity and pore size distribution can be used to obtain information on performance of cement based materials including concrete. However, porosity and pore size distribution are governed by factors like w/c ratio, age and size of cement or cementitious particles etc (Kondraivendhan and Bhattacharjee 2010).

In this study, crushed concrete chunk samples were tested by using MIP and pore size distribution parameters of concrete such as mean distribution radius ( $r_{0.5}$ ), porosity ( $P$ ) and dispersion coefficient ( $d$ ) were deter-

<sup>1</sup>Assistant Professor, Applied Mechanics Department, S.V. National Institute of Technology, Surat, India  
E-mail: kondraivendhan78@yahoo.co.in

<sup>2</sup>Research Fellow, School of Civil and Environmental Engineering, Nanyang Technological University, Singapore.

<sup>3</sup>Associate Professor, School of Civil and Environmental Engineering, Nanyang Technological University, Singapore.

mined. The dispersion of pores in a porous cement based matrix is generally represented by 'd' (Kondraivendhan and Bhattacharjee 2010). By using these PSD parameters the compressive strength, permeability and hydraulic diffusivity were also estimated through the readily available compressive strength, permeability and hydraulic diffusivity relationships in the literature.

## 2. Experimental Investigation

The main purpose of this investigation was to estimate the compressive strength, permeability and hydraulic diffusivity of pozzolana blended concrete through pore size distribution parameters. The experimental factors and their levels have been chosen accordingly as follows;

### 2.1 Materials

#### 2.1.1 Cement

To investigate the pore size distribution parameters of concrete one ordinary Portland cement (OPC) (ASTM Type II) was used; with a coarser mean particle diameter of 14.7  $\mu\text{m}$ . The particle diameters were determined by the laser based time of transition method using a particle size analyzer. The specific surface of the cement is 360  $\text{m}^2/\text{kg}$ . To maintain the uniformity and reliability of results for all the concrete mixes the cement is obtained from the same manufacturer.

#### 2.1.2 Sand

Natural river sand owing to their rounded shape was used in this work as it ensures better packing characteristics than the crushed sand. Locally available river sand having the fineness modulus value of 2.9 and specific gravity of 2.64 was used.

#### 2.1.3 Coarse Aggregate

Crushed 20-mm maximum size of graded aggregate of quartzite origin was used as coarse aggregate. Coarse aggregate has negligible water absorption and specific gravity of 2.77. The overall grading requirement of coarse aggregate is satisfying ASTM C 33-03 (American society for testing and materials).

#### 2.1.4 Silica Fume

Silica fume with a specific surface of 1800  $\text{m}^2/\text{kg}$  and specific gravity of 2.2 was used in this investigation. Silica fume was used as cement replacement material at 5, 10 and 15 weight % of cement throughout this inves-

tigation. The mean silica fume diameter was determined by using laser based particle size analyzer and is 28.5  $\mu\text{m}$ .

#### 2.1.5 Slag

Slag with a specific surface of 870  $\text{m}^2/\text{kg}$  and specific gravity of 2.9 was used for this investigation. Slag was used as cement replacement material at 10, 30 and 50 weight % of cement throughout this investigation. The mean diameter of slag was also determined by using laser based particle size analyser and is 9.2  $\mu\text{m}$ . The chemical properties of cement, silica fume and slag are given in **Table 1**.

### 2.2 Mix Proportions and experimental factors

In this investigation, mixes has been chosen over a range of water to cement ratios namely 0.4, 0.5, and 0.6 for OPC concrete, OPC with silica fume concrete and OPC with slag concrete mixes. The above concrete specimens are tested at 1, 3, 7, 28, 42 and 90 days of curing. Silica fume replacement levels are 5%, 10% and 15% by weight of cement and slag replacement levels are 10%, 30% and 50% by weight of cement replacement. The mix proportions of all the concrete mixes are presented in **Table 2**.

### 2.3 Sample preparation and preconditioning

The 100 mm concrete cubes were crushed with hammer at various curing ages and broken chunks from centre of specimen were collected. The collected samples were then immersed in isopropanol (anhydrous alcohol) to arrest further hydration. The samples were left in alcohol in desiccators for 10 days by which time the solvent would have penetrated in to the specimens ensuring hydration arrestation and a stable pore structure

Table 1 Chemical properties of cement, silica fume and slag.

Oxides	Cement	Silica Fume	Slag
	Content (%)	Content (%)	Content (%)
SiO <sub>2</sub>	63	92	36
Al <sub>2</sub> O <sub>3</sub>	21.5	2	9
Fe <sub>2</sub> O <sub>3</sub>	5.5	2	1
CaO	4.5	1	44
SO <sub>3</sub>	1	0.3	1
MgO	2	1	8
Other oxides	1.5	2	2.5
LOI	1	2.3	3.1

Table 2 Mix proportions of concrete mixes.

Mix designation	OPC			Silica fume					Slag				
	c1	c2	c5	sf1	sf2	sf3	sf4	sf5	sl1	sl2	sl3	sl4	sl6
w/c ratio	0.5	0.4	0.6	0.5	0.5	0.5	0.4	0.6	0.5	0.5	0.5	0.6	0.5
a/c ratio	3	3	4	3	3	3	3	3	3	3	4	4	3
Cement(kg/m <sup>3</sup> )	503	526	365	476	449	422	445	341.7	451	348	209	201	248.5
SF (kg/m <sup>3</sup> )	0	0	0	25	50	75	78	60.3	0	0	0	0	0
Slag(kg/m <sup>3</sup> )	0	0	0	0	0	0	0	0	50	150	209	201	248.5

(Feldman and Beaudoin 1991; Kumar and Bhattacharjee 2003). After isopropanol treatment, samples were vacuum dried by 24 hours and then samples were stored in sealed desiccators over silica gel until tested.

### 3. Testing procedure

Porosimetry test was performed in Micromeritics mercury Porosimeter having a pressure range of sub ambient to 60,000 psi (414 MPa). The contact angle and surface tension of mercury were assumed to be 140° and 0.484 N/m (Kumar and Bhattacharjee 2003; Cook and Hover 1993) respectively, for the vacuum dried samples. With this pressure, the smallest size of pore into which mercury can be intruded is 2 nm. The largest radius (pore size) that can be accounted for in the pore size distribution is 0.2 mm with sub ambient pressure filling apparatus. Three numbers of samples were tested for given concrete to ensure adequate accuracy of the MIP results representing particular mix proportion. The MIP results were obtained in the form of raw data representing cumulative intruded volume versus pressure data. Raw data so obtained were processed to obtain  $r_{0.5}$ , P and d as discussed in the next section.

#### 3.1 Determination of $r_{0.5}$ , P and d

##### 3.1.1 MMF Model Applicable to MIP results

The general form of MMF (Morgan Mercer Flodin) model as applied to intruded volume v/s pressure curves is as given below.

$$V = \frac{ab + c(p)^d}{b + (p)^d} \quad (1)$$

Where V is the cumulative intruded volume in cc/cc at p applied pressure in psi; a, b, c and d are the constants of the equation. "a" represent intercept on y axis when p equals to 0, hence, for "a" equals to 0 the curve passes through the origin and the equation 1, becomes Hill equation (Patil and Bhattacharjee 2008) "b" can be expressed as  $(p_{0.5})^d$ ,  $p_{0.5}$  being the value of pressure corresponding to half of the maximum intruded volume, "c" represents the maximum intruded volume approached asymptotically, as the pressure approaches infinity. Lastly, "d" is the shape coefficient of the curve, for "d" equals to 1, response curve is hyperbolic, and as the coefficient d increases the curve becomes increasingly sigmoidal, and steeper, further, the curve tends to become step function as "d" approaches infinity (Patil 2006). Thus variation of intruded volume with applied pressure, i.e. porosimetry curve is nearly completely explained by Hill's equation which is given below.

$$V = \frac{c(p)^d}{b + (p)^d} \quad (2)$$

Using Washburn's equation this cumulative intruded volume versus pressure curve, i.e., the equation 2 can be converted in to intrusion volume versus radius curve i.e.

cumulative pore size distribution curve and the general form of the pore size distribution curve which is proposed by Patil and Bhattacharjee (2008) is given in equation 3.

$$V = \frac{Pr_{0.5}^d}{r^d + r_{0.5}^d} \quad (3)$$

Where P is permeable porosity of the material,  $r_{0.5}$  is the mean distribution radius corresponding to  $P_{0.5}$  and d is the dispersion coefficient of pores. The  $r_{0.5}$ , P and d, for all the mixes were determined through the procedure adopted by Patil and Bhattacharjee (2008) and are briefly described below. By using the MIP, raw discrete digital data were acquired by machine software during experimental investigation, single complete data set of pressure versus intrusion volume, from pressure of 0.5 psi to 60,000 psi is obtained. All the data sets obtained for the replicates for a given experimental condition was combined. The average pressure versus volume intrusion curves for three replicates was obtained through least square fit of all the discrete digital data of the replicates combined together. This was done by using software available freely as demo version "Curve Expert 1.3" (Hyams 2006). The Morgan Mercer Flodin (MMF) model represented the best fit curve in all cases. Thus values of the dispersion coefficient d and permeable porosity P were obtained directly from the MMF model. Further, converting cumulative volume versus pressure curve to cumulative pore size distribution curve through Washburn's equation, the  $r_{0.5}$  value was obtained. Thus, the experimentally calculated  $r_{0.5}$ , d and permeable porosity (P) are given in Tables 3-5 for OPC, OPC with silica fume and OPC with slag concrete mixes respectively.

### 4. Results and discussion on experimentally obtained PSD parameters

The estimated values of  $r_{0.5}$ , P and d are given in the Tables 3-5 for OPC, OPC with silica fume and OPC with slag concrete mixes respectively. A close look in to the Tables 3-5 would reveal that the  $r_{0.5}$  value decreases with decrease in w/c ratio owing to better packing characteristics and decreases with an increase in curing ages as a result of continuous hydration and pore refinement for all the mixes. It is observed that the P value decreases with an increase in age for the same w/c ratio as a result of more degree of hydration and pore refinement. It is also observed that porosity value decreases with decrease in w/c ratio due to less water filled spaces unoccupied by the expanding cement gel. Further the d value increases with an increase in curing ages due to uniform pore sizes and decreases with an increase in w/c ratio as expected. All these pore size distribution parameter variations are further explained in the following section.

## 4.1 Variation of PSD Parameters with Age

### 4.1.1 Variation of $d$ with age

A careful look in to the **Tables 3-5** reveals that  $d$  values increase with an increase in age for concrete prepared with both silica fume and slag tends to attain nearly constant values with small deviation in some cases. These deviations can be attributed to experimental error. A similar behaviour is observed in case of cement concrete as well. Increase of  $d$  in all cases signifies the attainment of uniformity of pore sizes with age. Thus the dispersion range of pore size distribution narrows down with increasing age implying the increasing homogeneity of pore sizes. However at later ages this dispersion range stabilizes implying that no further increase takes place on increase of moist curing beyond some age. The behaviour exhibited by the concrete mixes with respect to variation of  $d$  with age can be understood as with increase in age more gel products are formed and these products occupy originally water filled space resulting in reduction of larger size of capillary pores. At some stage, the available entry to the intrudable pores is only gel pores. Therefore the dispersion range of pore sizes reduces as indicated by increasing  $d$  values nearly constant.

### 4.1.2 Variation of $r_{0.5}$ with Age

The **Tables 3-5** reveals that generally  $r_{0.5}$  reduces with age from 1-28 days thereafter it becomes nearly constant. With increase in age, continuous progression of hydration results in formation of solid products of hydration which occupies more volume than the original volume of the unhydrated cement. Thus median pore size tends to reduce with age. However, the solid products of hydration are porous with characteristic gel pores. Thus after the originally water filled space is occupied by solid products of hydration, the intrusion of mercury takes place only through gel pores. However, the above mentioned originally water filled space remains unoccupied at the time of hydration arrestation forms capillary pores through which intrusion of mercury takes place. At some instant of time hydration products become sufficient to disconnect the originally water filled space and thus the segmentation of capillaries takes place the pore segmentation, the median pore radius reduces drastically and mercury intrusion can take place only through gel pores.

### 4.1.3 Variation of Porosity with Age

The porosity reduces with an increase in curing ages continuously for concrete prepared with silica fume and slag. The behaviour is similar for cement concrete as well. In case of concrete, the porosity values are lower because of increasing the overall volume due to the intrusion of sand in the system. However, the reduction of porosity is not proportional to the volume of sand fraction present in the concrete, as fresh pores are created at the ITZ (Interfacial Transition Zone). Quantifying the ITZ porosity however, is difficult and the role of volume

Table 3 Experimental PSD parameters for OPC concrete.

Mix	w/c	age	PSD Parameters		
			P	$r_{0.5}$ nm	$d$
c1	0.5	1	0.178	5.31	0.757
c1	0.5	4	0.113	5.16	1.214
c1	0.5	28	0.096	4.85	1.489
c1	0.5	42	0.086	4.72	1.741
c2	0.4	4	0.091	3.82	1.215
c2	0.4	7	0.085	3.76	1.495
c5	0.6	7	0.180	5.86	1.264
c5	0.6	28	0.148	5.73	1.301

Table 4 Experimental PSD parameters for OPC with silica fume concrete.

Mix	w/c	% Silica Fume	age	PSD Parameters		
				P	$r_{0.5}$ nm	$d$
sf1	0.5	0.05	28	0.087	6.43	2.128
sf2	0.5	0.1	4	0.110	6.17	1.861
sf2	0.5	0.1	28	0.101	4.11	1.897
sf3	0.5	0.15	1	0.152	7.12	0.625
sf3	0.5	0.15	4	0.141	6.65	1.841
sf3	0.5	0.15	7	0.133	5.64	1.960
sf3	0.5	0.15	14	0.128	5.27	2.186
sf3	0.5	0.15	28	0.106	4.02	2.246
sf4	0.4	0.15	28	0.107	2.26	1.314
sf5	0.6	0.15	28	0.127	7.21	2.006

Table 5 Experimental PSD parameters for OPC with slag concrete.

Mix	w/c	% Slag	age	PSD Parameters		
				P	$r_{0.5}$ nm	$d$
sl-1	0.5	0.1	7	0.123	4.70	1.381
sl-1	0.5	0.1	28	0.104	2.37	1.144
sl-2	0.5	0.3	4	0.133	4.40	1.303
sl-2	0.5	0.3	28	0.112	1.31	0.863
sl-3	0.5	0.5	4	0.254	6.21	0.688
sl-3	0.5	0.5	7	0.212	4.04	0.778
sl-3	0.5	0.5	14	0.184	3.82	0.880
sl-3	0.5	0.5	28	0.152	2.15	0.892
sl-4	0.6	0.5	28	0.186	2.56	0.899
sl-6	0.5	0.5	1	0.254	5.28	1.129
sl-6	0.5	0.5	4	0.231	3.44	1.121

proportion of sand on the porosity can only be analyzed through an experimental scheme, where volume of sand content is varied in the paste. Such experimentation is not undertaken in the study and can be suggested as possible scope for further study. With intrusion of silica fume and slag in the cement concrete, the porosity reduces from 7 to 28 days and may be due to the creation of addition of gel products through pozzolanic reaction.

## 4.2 Variation of PSD Parameters with silica fume and slag

It is expected that the rate of hydration is faster in silica fume. The observed  $d$  values are given in **Table 4**. With regard to  $r_{0.5}$ , mix with 15% silica fume replacement has lower values of  $r_{0.5}$  than mix with 5% silica fume re-

placement. The  $r_{0.5}$  values are influenced by packing of the particulate system of cement and sand along with water. The packing characteristics and secondary pozzolanic reaction of 15% silica fume is more as compared to 5% silica fume mix. Thus concrete prepared with 15% silica fume tend to exhibit lower values of  $r_{0.5}$ . In case of slag concrete mixes, the  $r_{0.5}$  reduces at 30% replacement as compared to 10% replacement and again increases at 50% replacement. Thus it is not showing any systematic variation with respect to slag replacement in concrete mixes.

As seen from these tables, it is observed that the  $r_{0.5}$  and  $d$  values do not vary much even after 28 days of curing ages because of the substantial percentage of hydration is completed within this period. Mostly the  $r_{0.5}$  and  $d$  values become constant after 28 days of curing ages. The typical  $r_{0.5}$  versus age curves for c1, sf3 and sl3 mixes are given in Figs. 1-3 respectively. From these figures it is observed that  $r_{0.5}$  reduces with age and is asymptotic to x axis as well. The typical  $d$  versus age curves for c1, sf3 and sl3 mixes are given in Fig. 4. From this figure, it is observed that  $d$  increases with an increase in curing ages as a result of progress of degree of hydration and is asymptotic to x axis as well.

### 5. Implication of estimated PSD parameters

#### 5.1 Compressive strength through PSD parameters

The most suitable relationship available in the literature between strength and pore size distribution parameters (mean distribution radius and porosity) is considered (Kumar and Bhattacharjee 2003; Atzeni *et al.* 1987; Das and Kondraivendhan 2012). The  $r_{0.5}$  and  $P$  are estimated from mix factors such as w/c ratio, age, and mean cement particle diameter through the relationships. Porosity and pore sizes govern the strength of cement based materials. It is demonstrated that strength of cement based material is linearly related to  $(1-P)/\sqrt{r_{0.5}}$  with no intercept in y axis (Kumar and Bhattacharjee 2003; Atzeni *et al.* 1987; Das and Kondraivendhan 2012), where  $P$  is the porosity and  $r_{0.5}$  is mean distribution radius. The constant of proportionality of the above linear relationship is related to properties of pore free solid. Further as an extension of the above concept  $c(1-P)/\sqrt{r_{0.5}}$  is shown to be linearly related to in-situ strength of concrete. 'c' the cement content of the concrete mix, expressed as fraction. It is incorporated in the equation as properties of the pore free solid matrix, namely, the modulus of elasticity and surface energy, depend on the binder content.  $r_{0.5}$  is in nano-meter and strength is in MPa. Thus compressive strength  $\sigma$  can be written in terms of  $r_{0.5}$  and  $P$  as

$$\sigma = Kc \frac{(1-P)}{\sqrt{r_{0.5}}} \tag{4}$$

Where,  $K$  is the constant of proportionality. But in

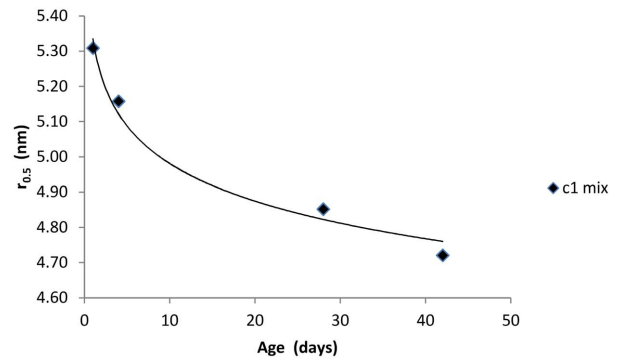


Fig.1  $r_{0.5}$  versus curing age for c1 mix with w/c ratio 0.5.

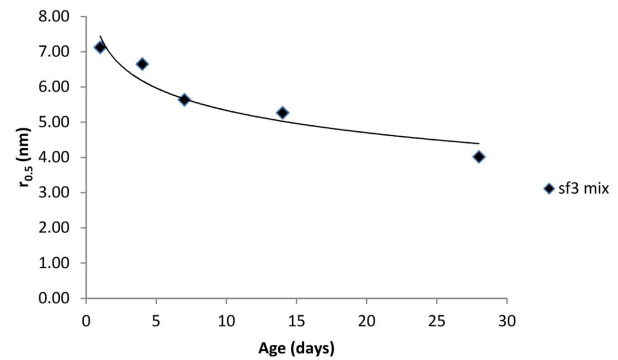


Fig.2  $r_{0.5}$  versus curing age for sf3 mix with w/c ratio 0.5.

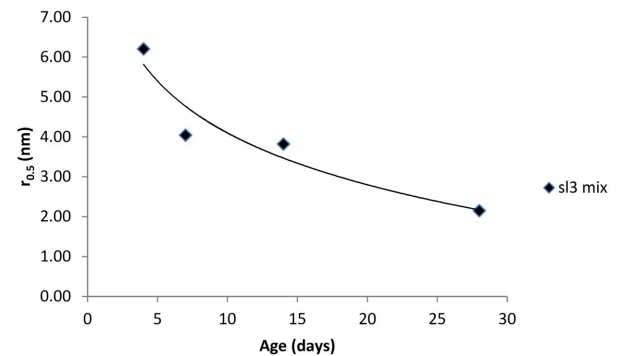


Fig.3  $r_{0.5}$  versus curing age for sl3 mix with w/c ratio 0.5.

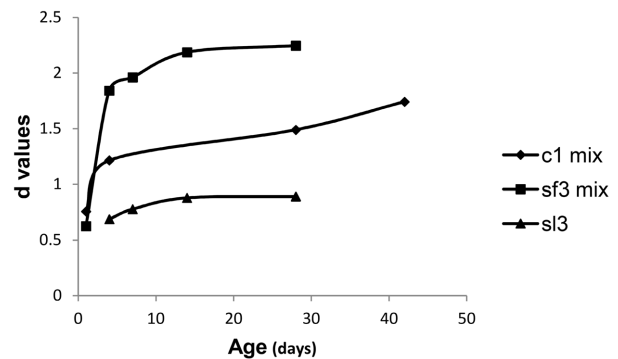


Fig.4  $d$  versus age for concrete mixes.

this investigation concrete mixes consist of cement with pozzolana materials such as silica fume and slag. So the above relationship is slightly modified as

$$\sigma = K(c+m) \frac{(1-P)}{\sqrt{r_{0.5}}} \tag{5}$$

Where, m is pozzolana content in the concrete mix. To determine the constant of proportionality of this relationship, the experimental compressive strength is plotted against the corresponding (c+m)(1-P)/sqrt(r<sub>0.5</sub>). Thus the K value obtained is 560.71 and the coefficient of correlation is 80%. The compressive strength versus (c+m) (1-P)/sqrt(r<sub>0.5</sub>) plot is presented in Fig. 5.

**5.2 Permeability and hydraulic diffusivity through PSD parameters**

Porosity and pore sizes govern the permeability of cement based materials as well. Pradhan *et al.* (2005) proposed a model for permeability and hydraulic diffusivity of concrete with pore size distribution parameters as an input. The value of hydraulic diffusivity is more during wetting as compared to that of drying. Using the hydraulic diffusivity model the variation of hydraulic diffusivity with relative water content is determined for two cases viz. 1) ideal continuous wetting and 2) ideal continuous drying. Expressions for hydraulic conductivity K(θ) is given below.

$$K(\theta) = \frac{pr_{0.5}^2 \rho g}{12\mu\tau^2(1+1/\alpha^2)} \tag{6}$$

Where p is porosity, r<sub>0.5</sub> is mean distribution radius in nm, ρ is density of water in kg/m<sup>3</sup>, g is the acceleration due to gravity in m/s<sup>2</sup>, μ is viscosity of water in N-s/m<sup>2</sup>, τ is tortuosity and α is the aspect ratio. In saturated condition, the hydraulic conductivity is referred as permeability. Thus the permeability is estimated for all the concrete mixes considered in this investigation and are given in Tables 6-8. The estimated permeability increases with an increase in w/c ratio and decreases with an increase in curing ages as a result of extended degree of hydration and particularly due to secondary pozzolanic reactions in case of OPC with silica fume and OPC with slag mixes. Thus, the nature of variation of permeability with respect to w/c ratio resembles the Powers' permeability versus w/c ratio curves (Neville

and Brooks 1990).

The implication of pore size distribution parameters of concrete are also extended to hydraulic diffusivity. First the permeability is estimated in the same manner as described above for both wetting and drying cases and the corresponding suction head is also estimated by using the reported relationship for suction head in the literature (Pradhan *et al.* 2005). In case of continuous wetting the pores are filled starting from the largest sized pores first, followed by smaller size pores progressively with increase in water content, such that the least water content corresponds to the largest pores (Pradhan *et al.* 2005). Whereas in the case of continuous drying the saturated pores is first emptied starting from the largest sized pores followed by the emptying of smaller sized pores progressively as the water content decreases, such that the least water content corresponds

Table 6 Estimated permeability for OPC concrete.

Mix	w/c	Age (days)	Permeability m/s
c1	0.5	1	6.84E-13
c1	0.5	4	6.46E-13
c1	0.5	28	5.72E-13
c1	0.5	42	5.41E-13
c2	0.4	4	3.62E-13
c2	0.4	7	3.51E-13
c5	0.6	7	6.70E-13
c5	0.6	28	6.41E-13

Table 7 Estimated permeability for OPC with silica fume concrete.

Mix	w/c	% Silica Fume	Age (days)	Permeability m/s
sf1	0.5	0.05	28	3.93E-13
sf2	0.5	0.1	4	4.58E-13
sf2	0.5	0.1	28	1.87E-13
sf3	0.5	0.15	1	8.41E-13
sf3	0.5	0.15	4	6.79E-13
sf3	0.5	0.15	7	4.61E-13
sf3	0.5	0.15	14	3.88E-13
sf3	0.5	0.15	28	1.86E-13
sf4	0.4	0.15	28	5.96E-14
sf5	0.6	0.15	28	7.22E-13

Table 8 Estimated permeability for OPC with slag concrete.

Mix	w/c	% Slag	Age (days)	Permeability m/s
sl-1	0.5	0.1	7	7.76E-15
sl-1	0.5	0.1	28	2.80E-15
sl-2	0.5	0.3	4	8.50E-15
sl-2	0.5	0.3	28	1.80E-15
sl-3	0.5	0.5	4	4.38E-14
sl-3	0.5	0.5	7	1.99E-14
sl-3	0.5	0.5	14	1.41E-14
sl-3	0.5	0.5	28	5.43E-15
sl-4	0.6	0.5	28	9.68E-15
sl-6	0.5	0.5	1	3.72E-14
sl-6	0.5	0.5	4	2.00E-14

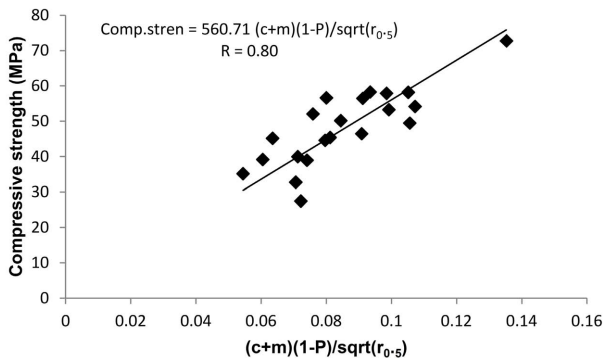


Fig.5 Compressive strength versus (c+m)(1-P)/sqrt(r<sub>0.5</sub>) plot for concrete.

to the smallest pore sizes. From the definition, the hydraulic diffusivity is obtained as the ratio of hydraulic conductivity to specific water capacity. The model for hydraulic diffusivity is as follows:

$$D(\theta) = \frac{f \sigma_w \cos \phi \times p_j r_{0.5j}}{3\pi\rho\mu\tau^2 r_j^2 \left(\frac{dv}{dr}\right)_j (1+1/\alpha^2)} \quad (7)$$

Where,  $f$  is the multiplying correction factor for shape,  $\sigma_w$  is surface tension of water in N/m,  $\phi$  is contact angle for water and rest of notations have the same meaning as stated earlier. The hydraulic diffusivity is considered to be dependent on degree of saturation or relative moisture content. A typical hydraulic diffusivity versus relative moisture content for both wetting and drying cases are given in Fig. 6. It follows the similar trend as given by Pradhan *et al.* (2005). The profile of hydraulic diffusivity with relative moisture content during wetting and drying represent the upper and lower bounds of hydraulic diffusivity. All the practical values of hydraulic diffusivity are likely to lie within these bounds including the experimentally obtained variation of hydraulic diffusivity with relative water content.

## 6. Discussion

Determination of strength, permeability and hydraulic diffusivity through porosimetry is a very innovative method as compared to conventional way of determining compressive strength and permeability. It is also highlighted that pore size distribution parameters are functions of mix factors such as w/c ratio and age (Kondraivendhan and Bhattacharjee 2010). Even though strength and permeability obtained from porosimetry is not as same as conventional strength and permeability, it sounds good. The coefficient of correlation in case of strength is 80% (many more data are required to get still better correlations which are not available at present). The nature of variation of permeability with respect to w/c ratio also resembles the Powers' permeability versus w/c ratio curves (Neville and Brooks 1990). In this investigation, pore size distribution parameters are directly calculated from the porosimetry results. But one can improve this by modelling the pore size distribution parameters as a function of w/c ratio and age. Similar kind of work has been carried out by one of the author for OPC paste (Kondraivendhan and Bhattacharjee 2010). In future, this research would be extended to concrete and most probably better comparison could be obtained.

Concrete is a composite having coarse aggregate, fine aggregate and hardened paste in its finally set state. The pore size distribution of concrete is influenced by characteristics and volumetric concentration of aggregates (both fine and coarse aggregates). Therefore, the investigation on PSD of concrete would require choice of aggregates and its volumetric concentration as experi-

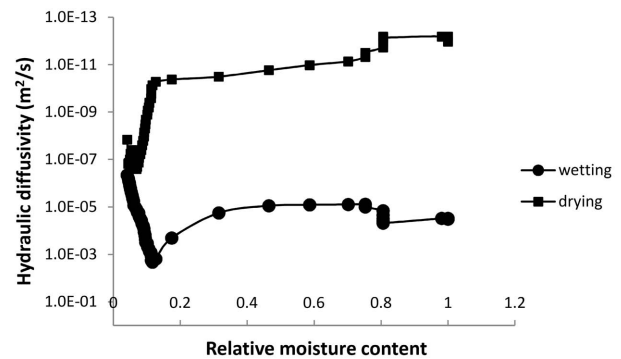


Fig.6 Hydraulic diffusivity against relative moisture content curve for sf3 mix.

mental factors and their several levels making the scope of the work unmanageable over a limited duration of time. So, the modelling of pore size distribution parameters was not done in this investigation. The  $K$  value could be improved by having more experimental data in further investigations.

The equations 5 and 6 are taken from the reported literature (Pradhan *et al.* 2005) and both are functions of pore size distribution parameters. It is known that the microstructure of pozzolona blended concrete is different from the normal OPC concrete. The pores are refined better in pozzolona blended concrete and the corresponding tortuosity and connectivity of pores are different from OPC concrete. Even though the pozzolona blended concrete tortuosity is dissimilar to OPC concrete, it is not taken in to account and the same tortuosity used for OPC concrete is followed in this investigation as well. The equations 5 and 6 are basic equations applicable to any cement based components. Thus, in case of pozzolona blended concrete, the pore size distribution parameters are obtained from the porosimetry results and applied in the corresponding equations while calculating the strength, permeability and hydraulic diffusivity.

## 7. Conclusions

Based on this experimental investigation and analysis, the following conclusions are drawn:

1. The lowest mean distribution radius is observed in case of OPC with silica fume mix as compared to other mixes as a result of extended degree of hydration of the mixture.
2. The dispersion coefficient is high in case of OPC with silica fume mix as compared to other mixes due to secondary pozzolanic reaction and better packing characteristics.
3. The compressive strength, permeability and hydraulic diffusivity of OPC with or without pozzolona blended concrete can be estimated through the pore size distribution parameters.
4. The estimated permeability increases with an increase in w/c ratio and decreases with an increase in curing ages which resembles trend of Powers' per-

meability versus w/c ratio curves.

5. The hydraulic diffusivity versus relative moisture content in both wetting and drying cases exhibits similar trend as reported in the literature.

## References

- American society for testing and materials for standard specifications for concrete aggregates, ASTM: C 33-03.
- Atzeni, C., Massidda, L. and Sanna, V., (1987). "Effect of pore size distribution on strength of hardened cement pastes." *Proceedings of the first International RILEM congress on Pore Structure and Material properties*, Paris, 195-202.
- Bhattacharjee, B. and Krishnamoorthy, S., (2004). "Permeable porosity and thermal conductivity of construction materials." *ASCE Journal of Materials in Civil Engineering*, 16(4), 322-330.
- Cook, R. A. and Hover, K. C., (1993). "Mercury porosimetry of cement based materials and associated correction factors." *Construction and Building Materials*, 7(4), 231-240.
- Das, B. B. and Kondraivendhan, B., (2012). "Implication of pore size distribution parameters on compressive strength, permeability and hydraulic diffusivity of concrete." *Construction and Building Materials*, 28(1), 382-386.
- Feldman, R. F. and Beaudoin, J. J., (1991). "Pre-treatment of hardened hydrated cement pastes for mercury intrusion measurements." *Cement and Concrete Research*, 27, 297-308.
- Hyams, D. G., (2006). "Curve Expert 1.3 a comprehensive curve fitting package for Windows 2005." [www.curveexpert.webhop.biz](http://www.curveexpert.webhop.biz).
- Kondraivendhan, B. and Bhattacharjee, B., (2010). "Effect of age, w/c ratio on size and dispersion of pores in ordinary portland cement paste." *ACI Materials Journal*, 107(2),147-154.
- Kumar, R. and Bhattacharjee, B., (2003). "Porosity, pore size distribution and in situ strength of concrete." *Cement and Concrete Research*, 33(1), 155-164.
- Kumar, R. and Bhattacharjee, B., (2003). "Study on some factors affecting the results in the Use of MIP method in concrete research." *Cement and Concrete Research*, 33, 417-424.
- Kumar, R. and Bhattacharjee, B., (2004). "Assessment of permeation quality of concrete through mercury intrusion porosimetry." *Cement and Concrete Research*, 34(2), 321-328.
- Nagaraj, T. S. and Zahinda, B., (1996). "Generalization of abrams law." *Cement and Concrete Research*, 26(6), 993-942.
- Neville, A. M. and Brooks, J. J., (1990). "Concrete technology." ELBS Edition, Longman Singapore, Publishers, (Pte). Ltd.
- Patil, S. G., (2006). "A study on porosity and pore size distribution obtained through MIP of cement paste and cement sand mortar incorporating silica fume." PhD Thesis IIT Delhi.
- Patil, S. G. and Bhattacharjee, B., (2008). "Size and volume relationship of pore for construction materials." *ASCE Journal of Materials in Civil Engineering*, 20(6), 410-418.
- Pradhan, B., Nagesh, M. and Bhattacharjee, B., (2005). "Prediction of the hydraulic diffusivity from pore size distribution of concrete." *Cement and Concrete Research*, 35(9),1724-1733.